In silico strategy for isoform-selective 5-HT_{2A}R and 5-HT_{2C}R inhibitors

Xiaohui Geng[a], Ying Wang[b], Huibin Wang[a], Baichun Hu[c,d], Junhao Huang[a], Yiheng Wu[c,d], Jian Wang[c,d], Fengjiao Zhang[b*]

a. School of Pharmacy, Shenyang Pharmaceutical University, Shenyang 110016, People's Republic of China

b. Wuya College of Innovation, Shenyang Pharmaceutical University, Shenyang 110016, People's Republic of China

c. Key Laboratory of Structure-Based Drug Design &Discovery of Ministry of Education, Shenyang Pharmaceutical University, Shenyang 110016, People's Republic of China

d. School of Pharmaceutical Engineering, Shenyang Pharmaceutical University, Shenyang 110016, People's Republic of China

Geng X. and Wang Y. contributed equally to this work.

Corresponding author: Prof. Fengjiao Zhang, E-mail: zhangfengjiao@syphu.edu.cn.

Table of contents

frame of MD simulations.

16. **Figure S16** The RMSD plot of 5-HT_{2A}R protein with single residue mutated to alanine.

17. **Figure S17** Normalized stacked bar charts of interactions and contacts throughout the course of MD simulations trajectory for mutated 5-HT_{2A}R complexes.

18. **Figure S18** The RMSD plot of 5-HT_{2C}R protein with single residue mutated to alanine.

19. **Figure S19** Normalized stacked bar charts of interactions and contacts throughout the course of MD simulations trajectory for mutated 5-HT_{2C}R complexes.

20. **Figure S20** The ROC curves and AUC resulting from the evaluation of the structure-based pharmacophore models generated from the investigated 5-$HT_{2A/C}$R complexes.

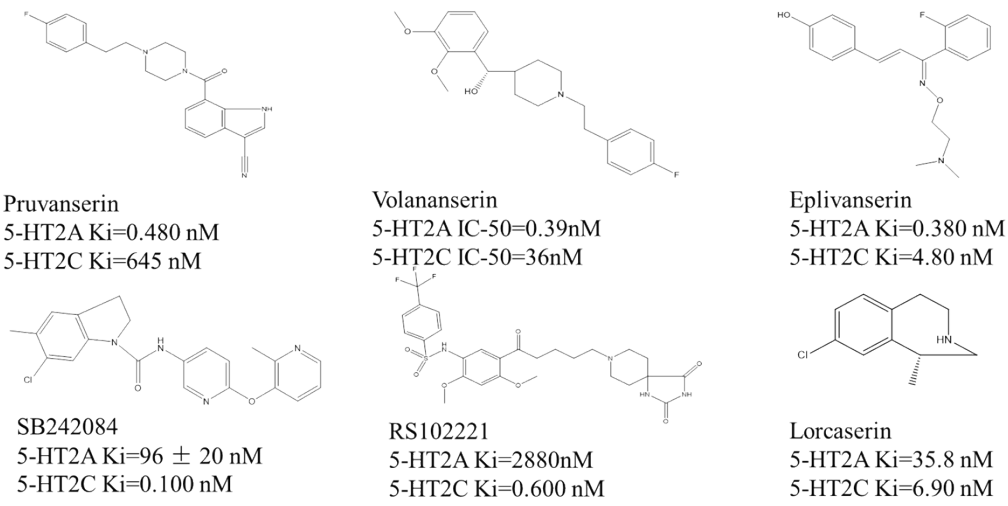

Figure S1 Chemical structures and bioactivities of 5-$HT_{2A/C}$ protein antagonists.

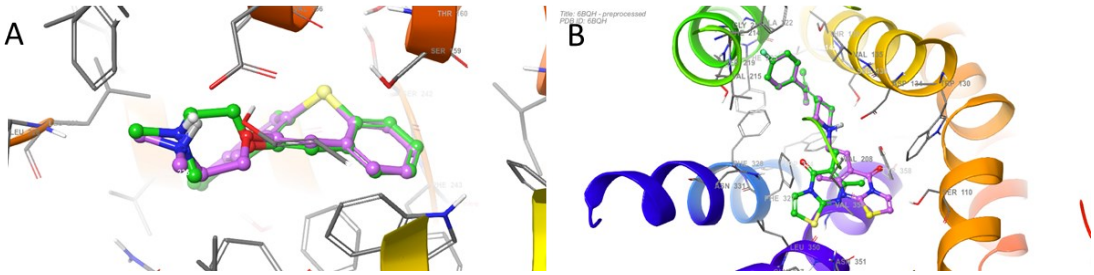

Figure S2 The Comparison between the co-crystal ligands and their predicted poses of 5-$HT_{2A/C}$R, where the experimentally determined and re-docked poses were shown in green and purple, respectively. (A) Re-docking pose of 5-HT_{2A}R (PDB ID: 6A94) with RMSD value of 0.782 Å. (B) Re-docking pose of 5-HT_{2C}R (PDB ID: 6BQH) with RMSD value at 0.678 Å.

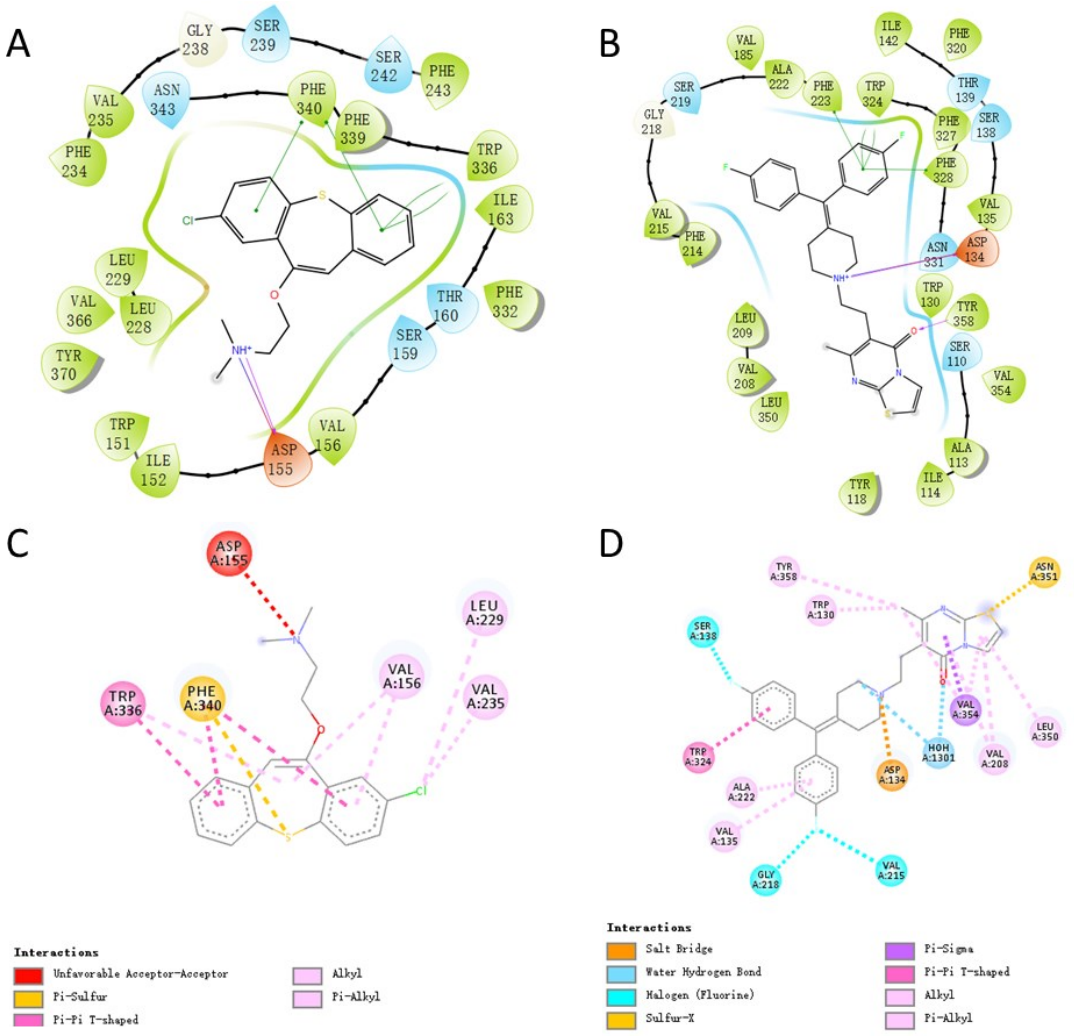

Figure S3 Two-dimensional diagrams of the receptor-ligand interaction represented in the co-crystal structures of 5-$HT_{2A/C}$R. (A) The binding pattern of 5-HT_{2A}R represented by Maestro program; (B)The binding pattern of 5-HT_{2C}R represented by Maestro program; (C) The binding pattern of 5-HT_{2A}R represented by Discovery Studio program; (D) The binding pattern of 5-HT_{2C}R represented by Discovery Studio program.

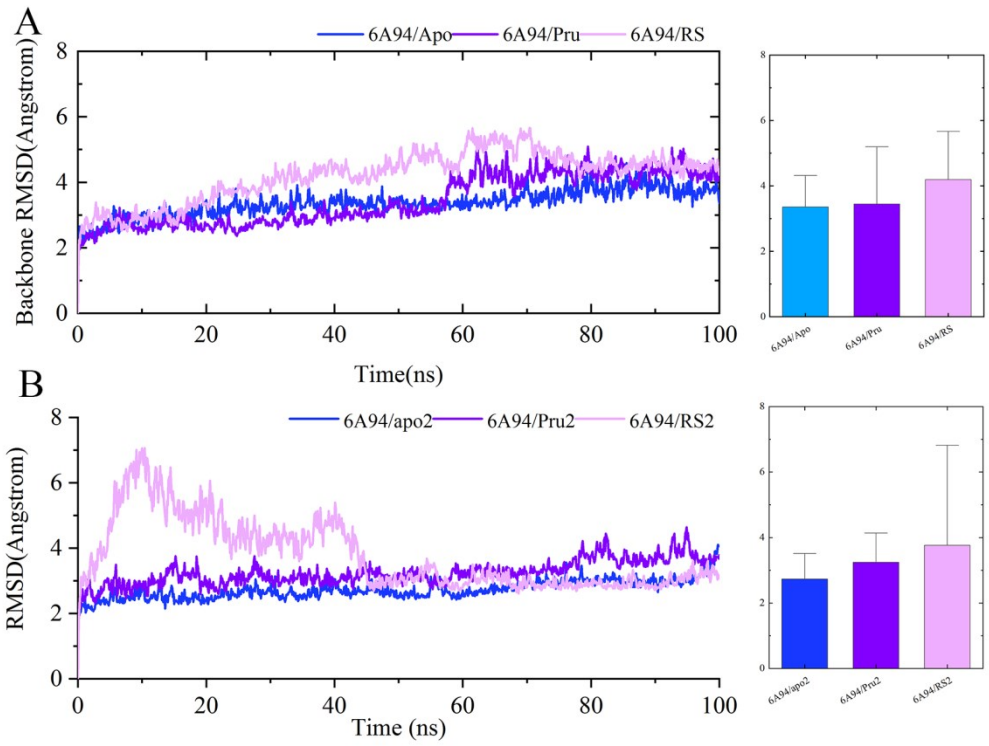

Figure S4 RMSD plots of 5-HT_{2A}R protein backbones from anther two sets of 100 ns MD simulations.

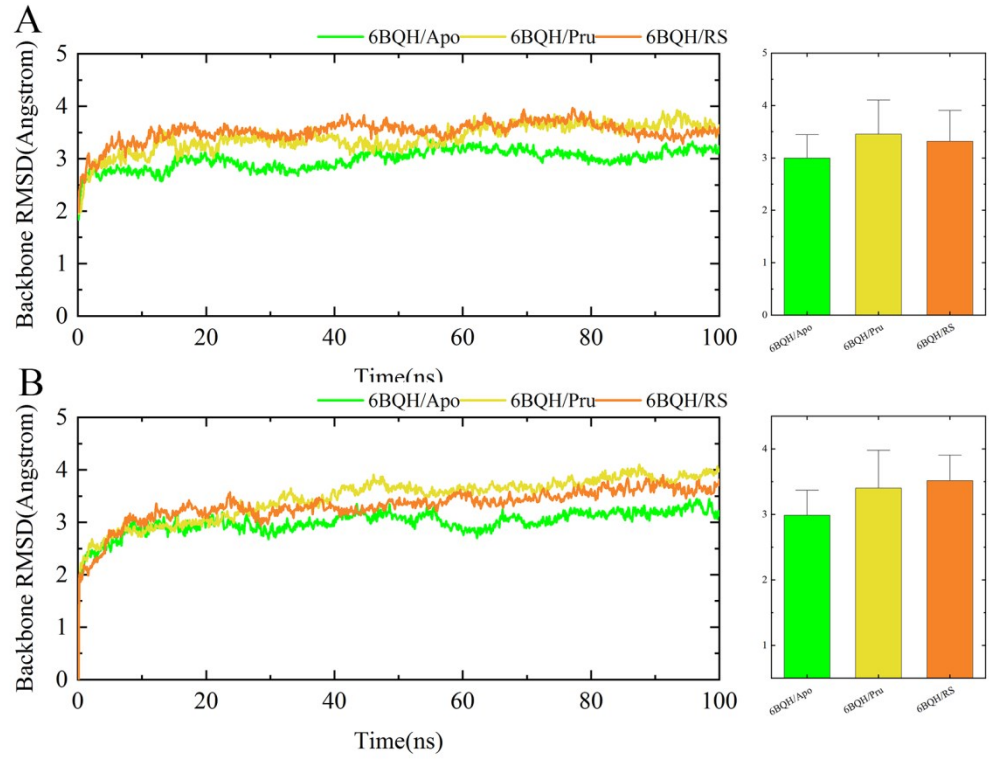

Figure S5 RMSD plots of 5-HT_{2C}R protein backbones from anther two sets of 100 ns

MD simulations.

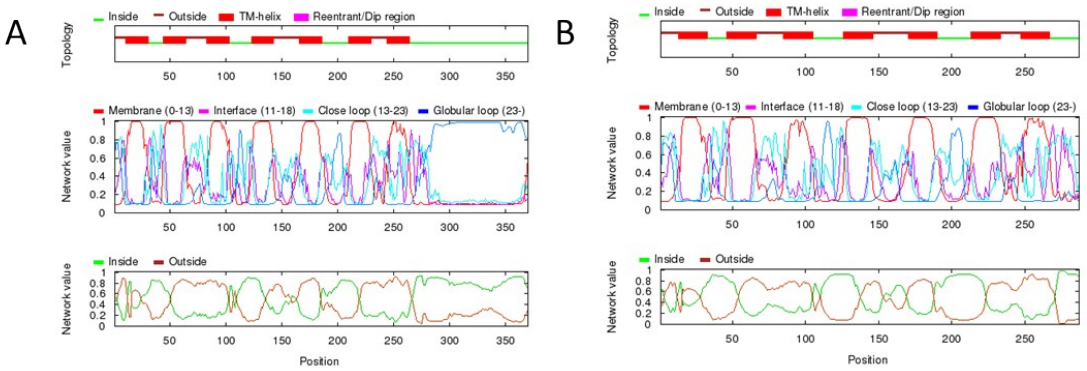

Figure S6 Transmembrane helices of 5-$HT_{2A/C}$R protein predicted by online program Octopus. (A) 5-HT_{2A} receptor, (B) 5-HT_{2C} receptor.

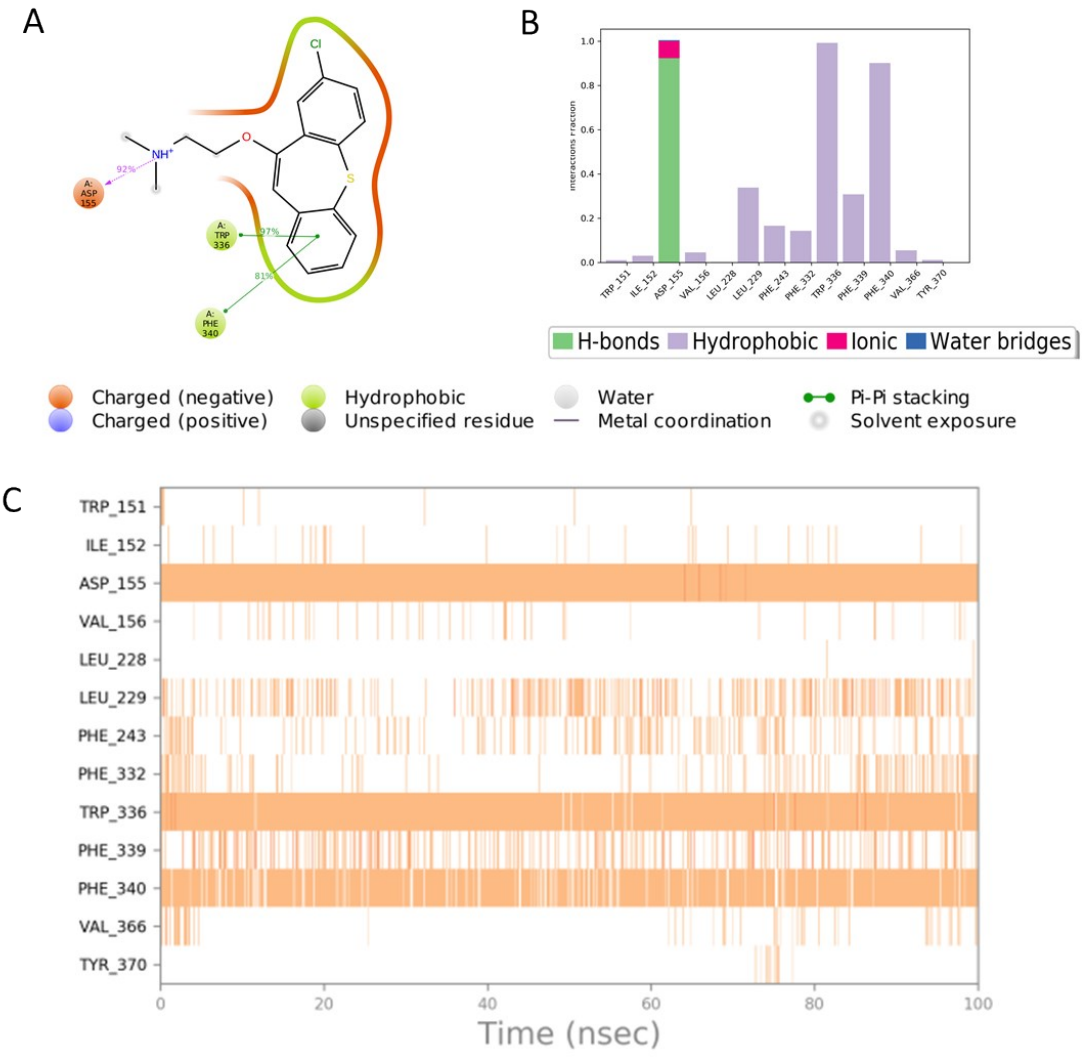

Figure S7 Protein-ligand interaction of 5-HT_{2A}R co-crystal complex monitored during the MD simulations. (A) The schematic of detailed ligand atom interactions with the protein residues. (B) The interaction fraction of each residue summarized into four categories summarized during the MD simulation. (C) The timeline representation of the receptor-ligand interactions during the MD simulation.

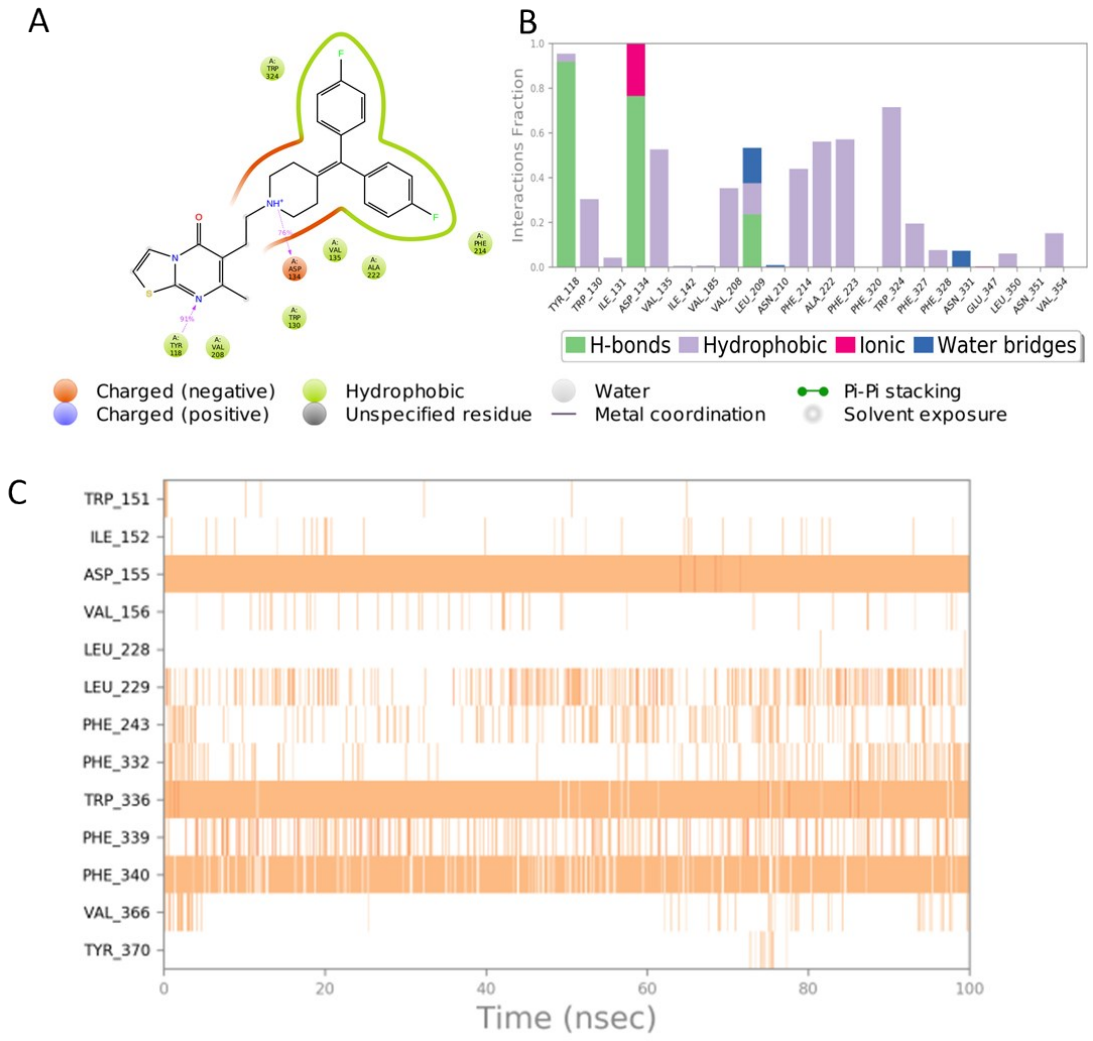

Figure S8 Protein-ligand interaction of 5-HT_{2C}R co-crystal complex monitored during the MD simulations. (A) The schematic of detailed ligand atom interactions with the protein residues. (B) The interaction fraction of each residue summarized into four

categories summarized during the MD simulation. (C) The timeline representation of the receptor-ligand interactions during the MD simulation.

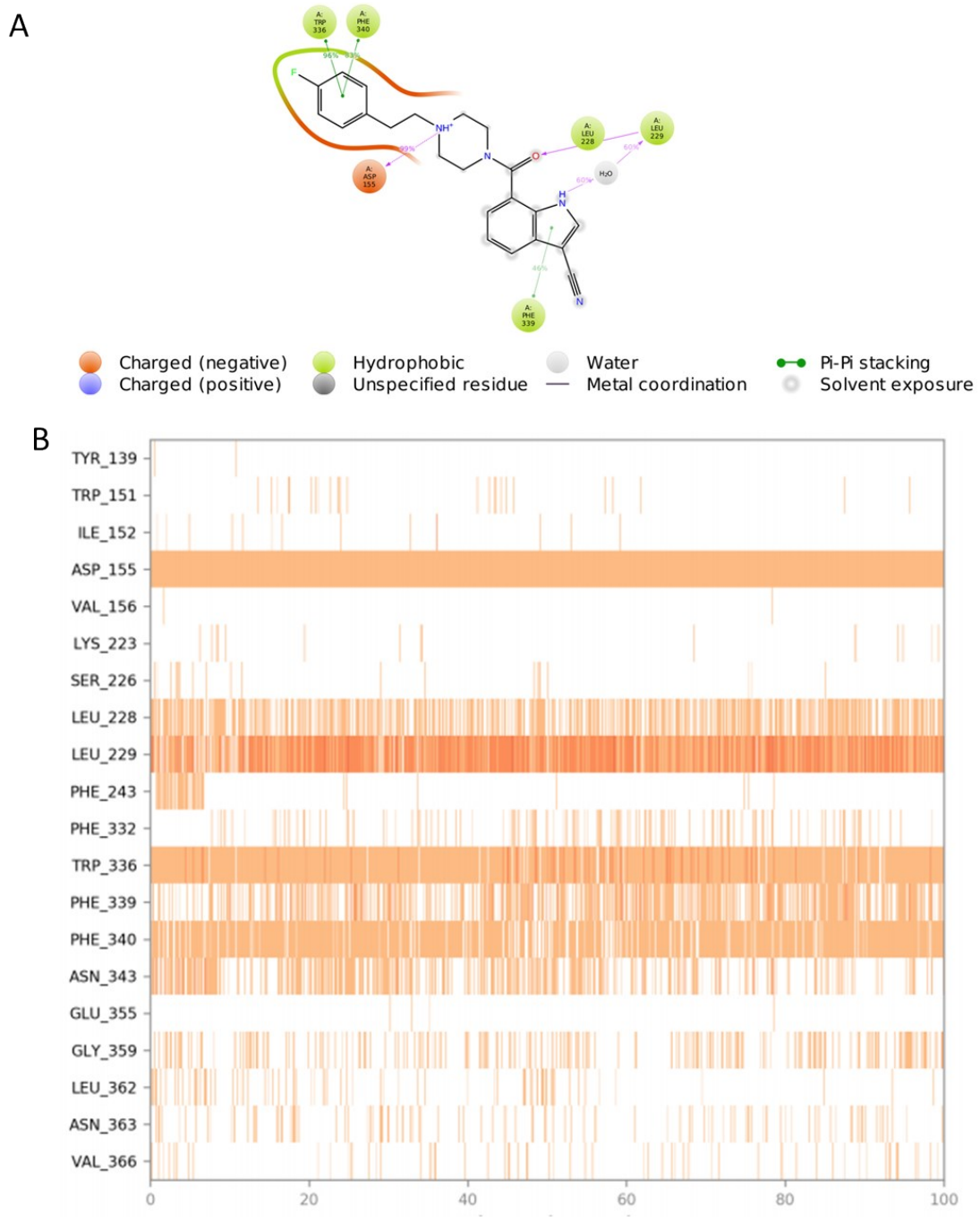

Figure S9 Protein-ligand interaction of 5-HT_{2A}R/Pruvanserin complex monitored during the MD simulations. (A) The schematic of detailed ligand atom interactions with the protein residues. (B) The timeline representation of the receptor-ligand interactions during the MD simulation.

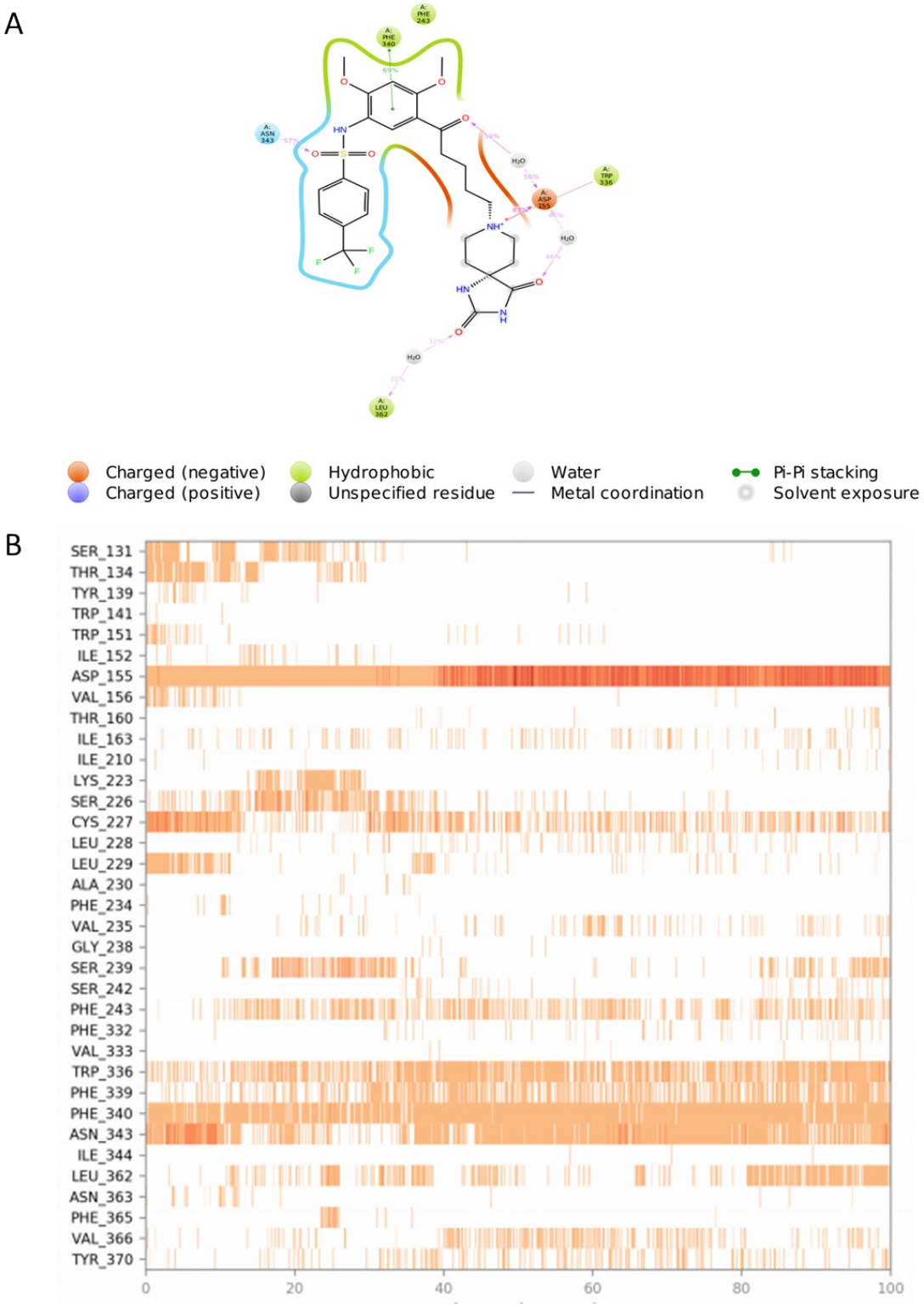

Figure S10 Protein-ligand interaction of 5-HT_{2A}R/RS102221 complex monitored during the MD simulations. (A) The schematic of detailed ligand atom interactions with the protein residues. (B) The timeline representation of the receptor-ligand interactions

during the MD simulation.

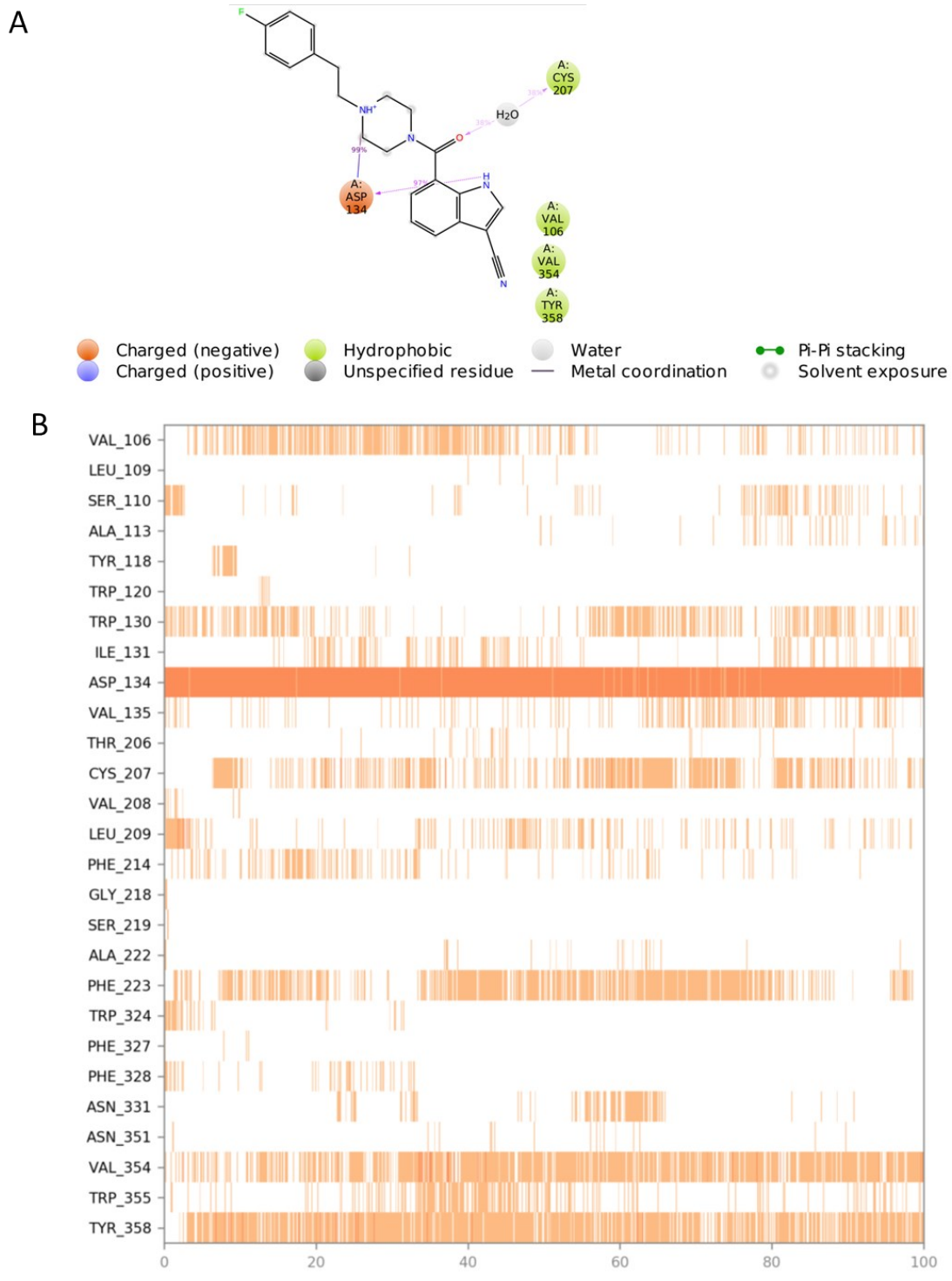

Figure S11 Protein-ligand interaction of 5-HT_{2C}R/Pruvanserin complex monitored during the MD simulations. (A) The schematic of detailed ligand atom interactions with the protein residues. (B) The timeline representation of the receptor-ligand interactions

during the MD simulation.

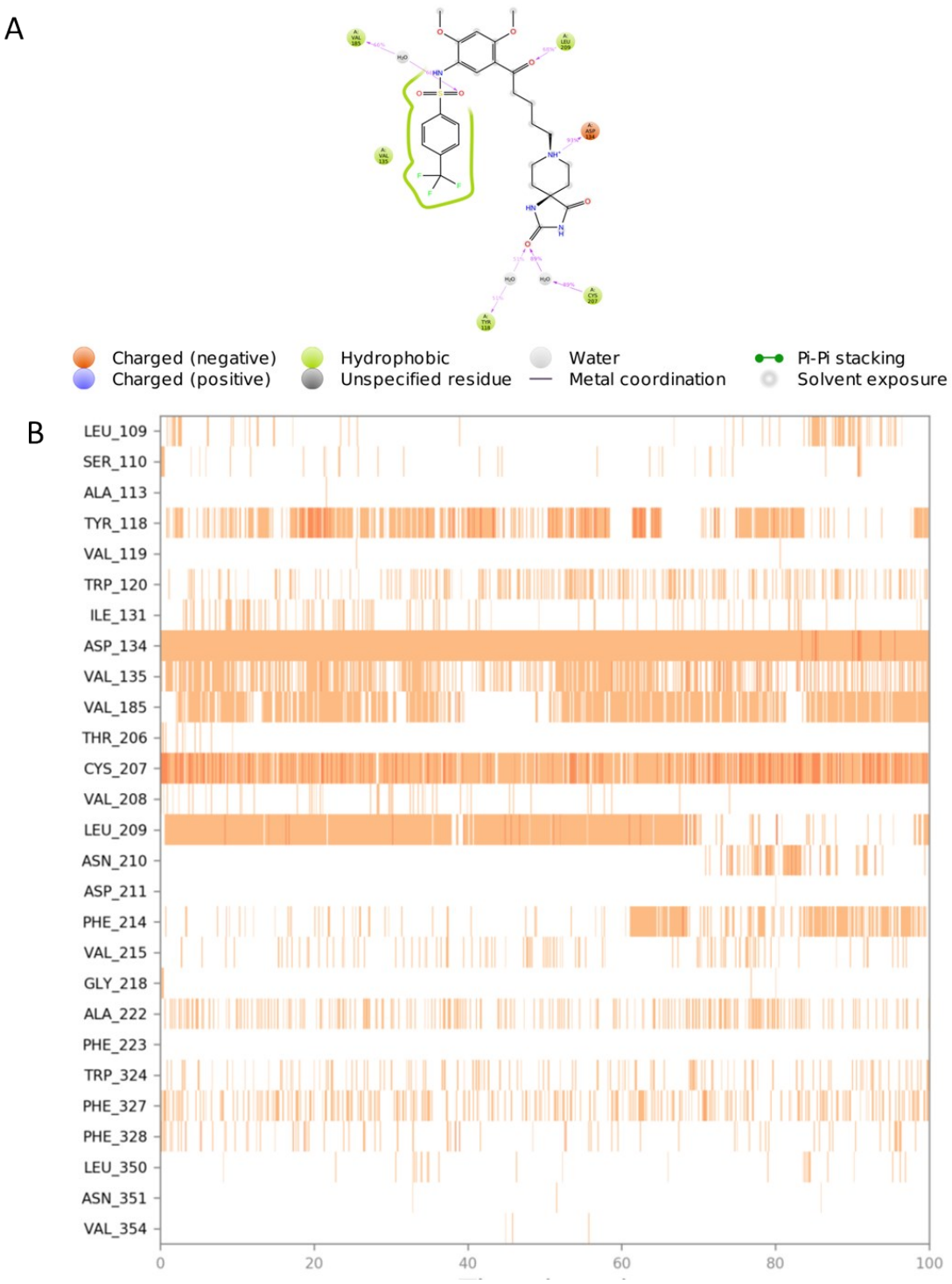

Figure S12 Protein-ligand interaction of 5-HT_{2C}R/RS102221 complex monitored during the MD simulations. (A) The schematic of detailed ligand atom interactions with the protein residues. (B) The timeline representation of the receptor-ligand interactions

during the MD simulation.

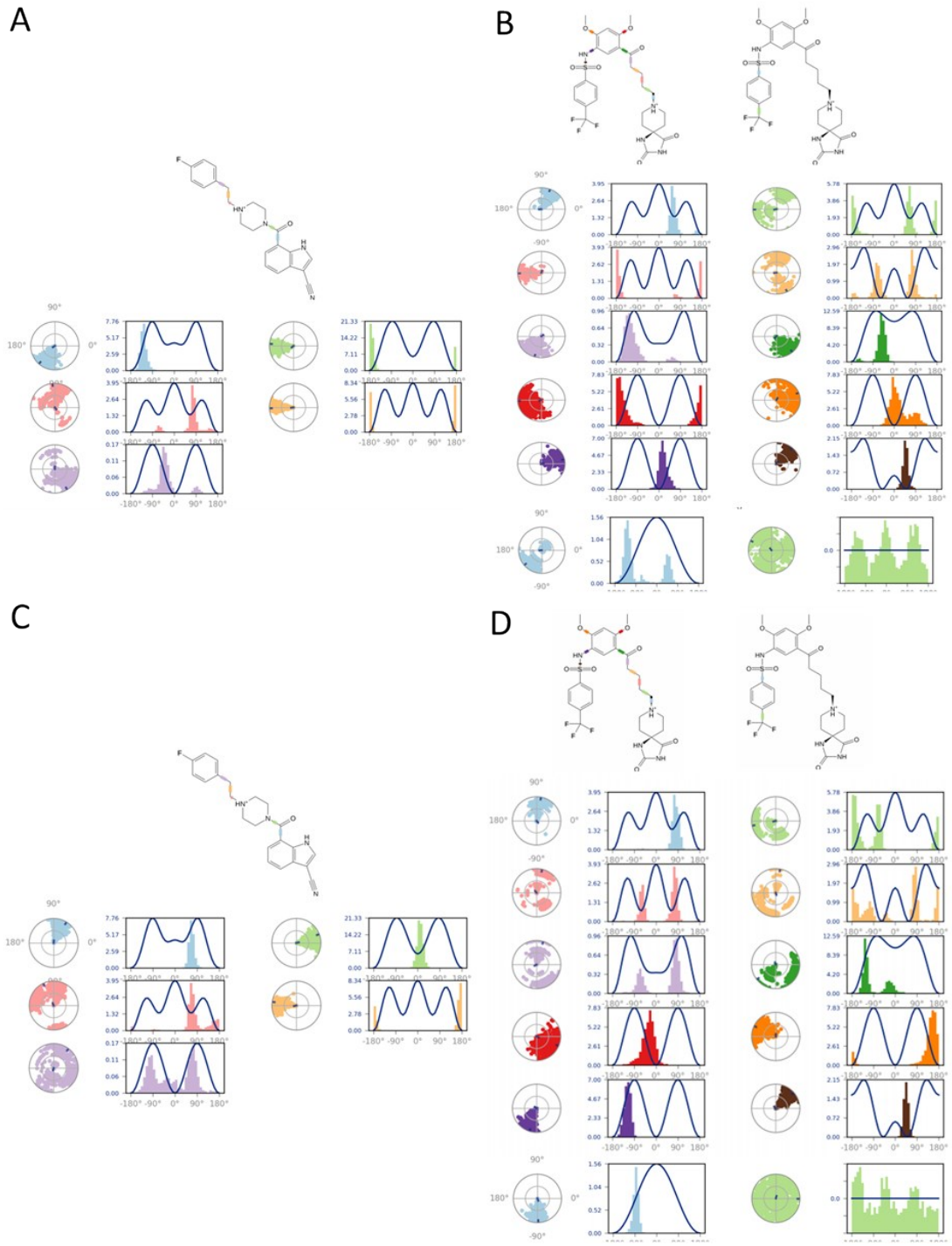

Figure S13 The ligand torsions plots of every rotatable bond in the ligand throughout the MD simulations. (A) 5-HT_{2A}R/Pruvanserin; (B) 5-HT_{2A}R /RS102221; (C) 5-HT_{2C}R/Pruvanserin; (D) 5-HT_{2C}R /RS10222.

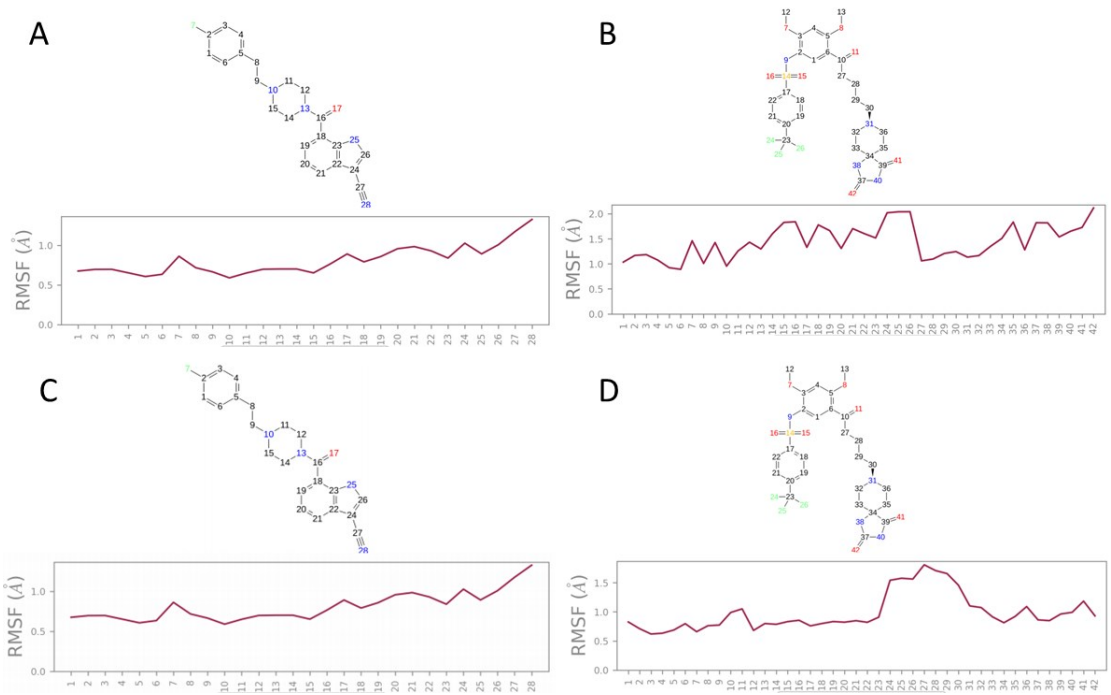

Figure S14 The ligand RMSF curves that characterize changes in the ligand atom positions during the 100 ns MD simulations. (A) Pruvanserin in 5-HT_{2A}R complex, (B) Pruvanserin in 5-HT_{2C}R complex, (C) RS102221 in 5-HT_{2A}R complex, (D) RS102221 in 5-HT_{2C}R complex.

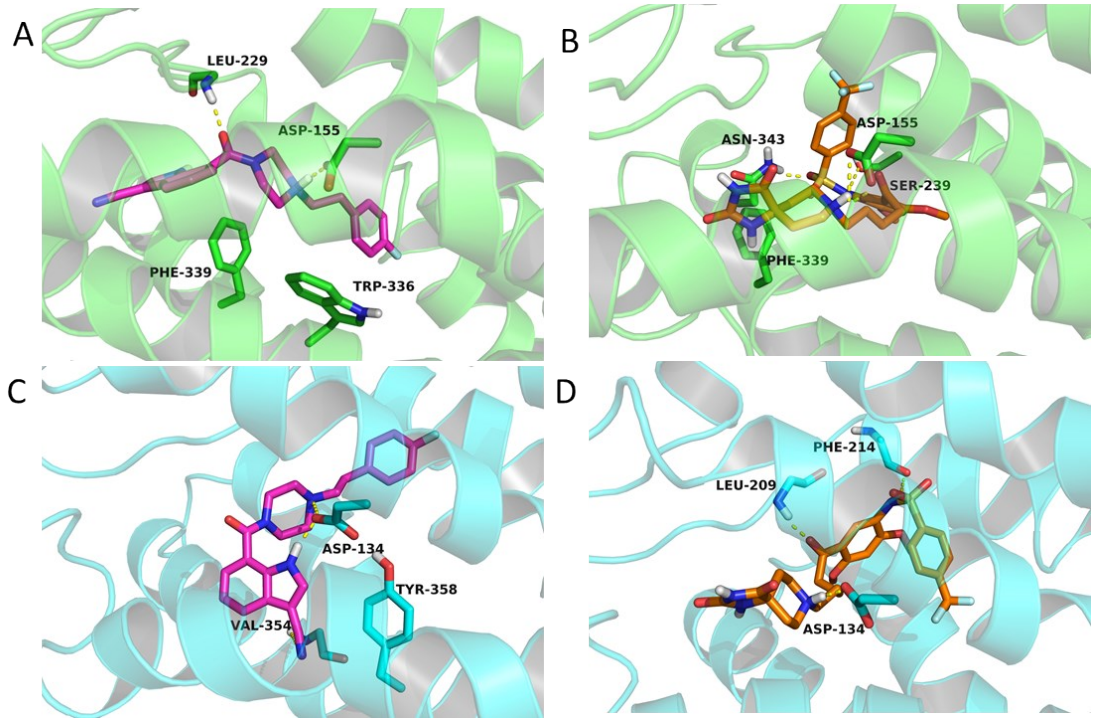

Figure S15 The binding modes of each investigated complex obtained from the last

frame of MD simulations, where the protein structures of 5-HT_{2A}R and 5-HT_{2C}R were represented in green and blue ribbon while the structures of Pruvanserin and RS102221 were represented in violet and orange sticks, respectively, and the hydrogen bonds were represented as yellow dashes. (A) 5-HT_{2A}R/Pruvanserin. (B) 5-HT_{2A}R/RS102221. (C) 5-HT_{2C}R/Pruvanserin. (D) 5-HT_{2C}R/RS102221.

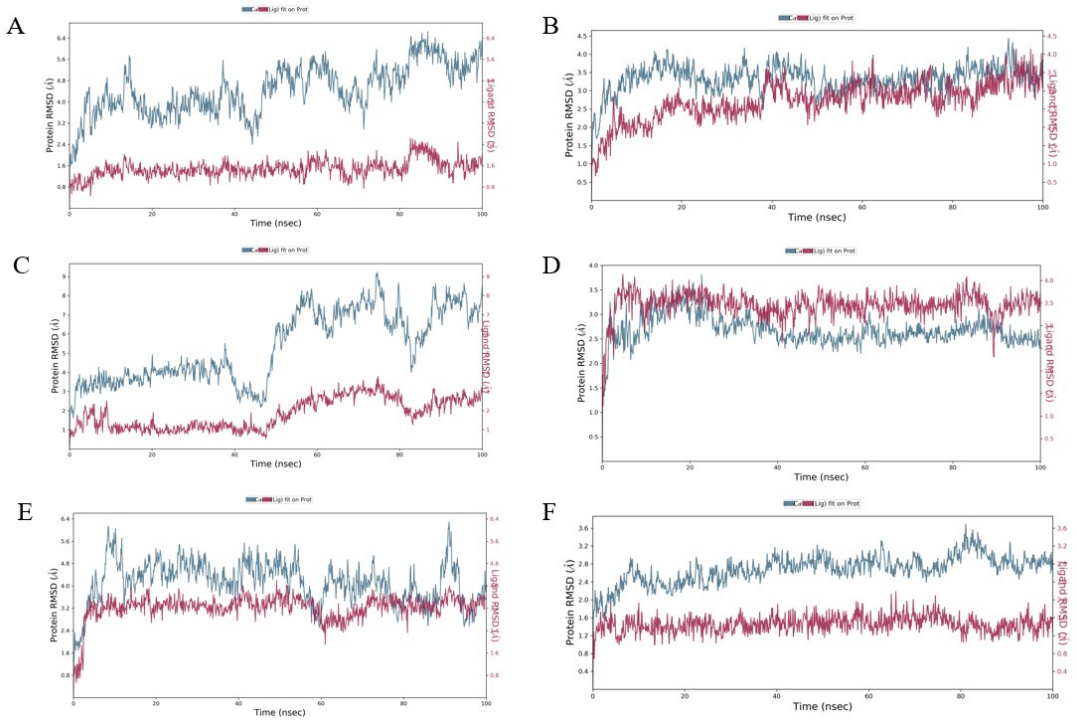

Figure S16 The RMSD plot of 5-HT_{2A}R protein with single residue mutated to alanine. (A) ASP155 mutated 5-HT_{2A}R/Pruvanserin complex. (B) TRP336 mutated 5-HT_{2A}R/Pruvanserin complex. (C) PHE340 mutated 5-HT_{2A}R/Pruvanserin complex. (D) ASP134 mutated 5-HT_{2A}R/RS102221 complex. (E) TRP336 mutated 5-HT_{2A}R/RS102221 complex. (F) PHE340 mutated 5-HT_{2A}R/RS102221 complex.

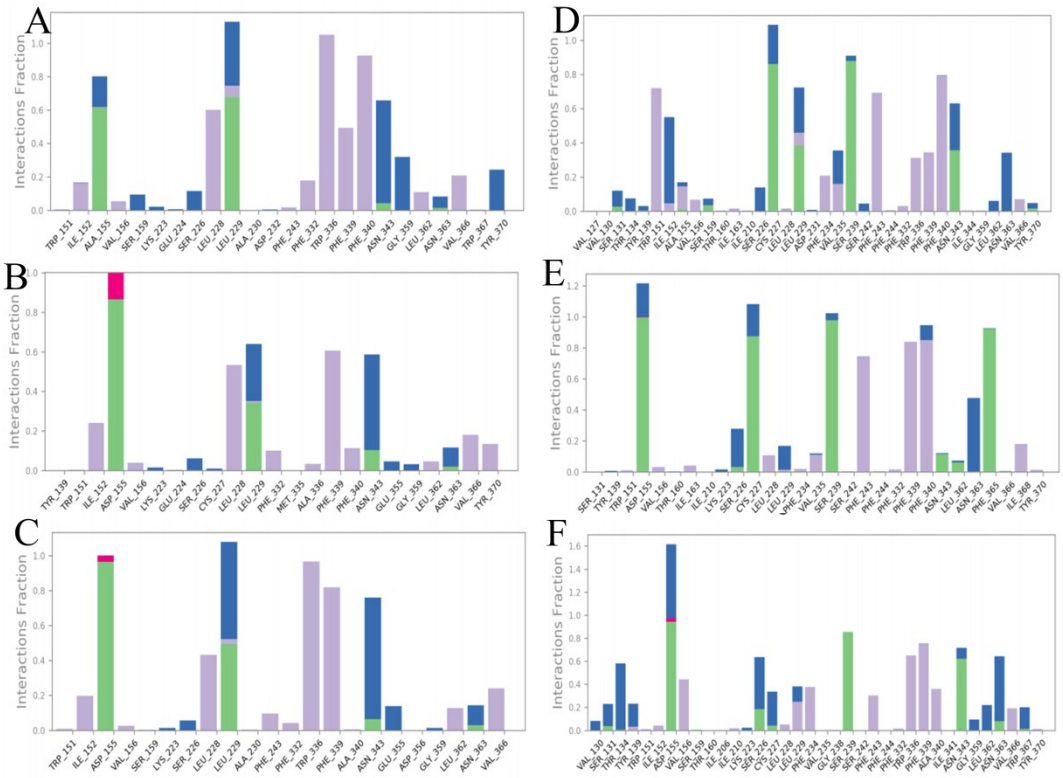

Figure S17 Normalized stacked bar charts of interactions and contacts throughout the course of MD simulations trajectory for mutated 5-HT_{2A}R complexes. (A) ASP155 mutated 5-HT_{2A}R/Pruvanserin complex. (B) TRP336 mutated 5-HT_{2A}R/Pruvanserin complex. (C) PHE340 mutated 5-HT_{2A}R/Pruvanserin complex. (D) ASP134 mutated 5-HT_{2A}R/RS102221 complex. (E) TRP336 mutated 5-HT_{2A}R/RS102221 complex. (F) PHE340 mutated 5-HT_{2A}R/RS102221 complex.

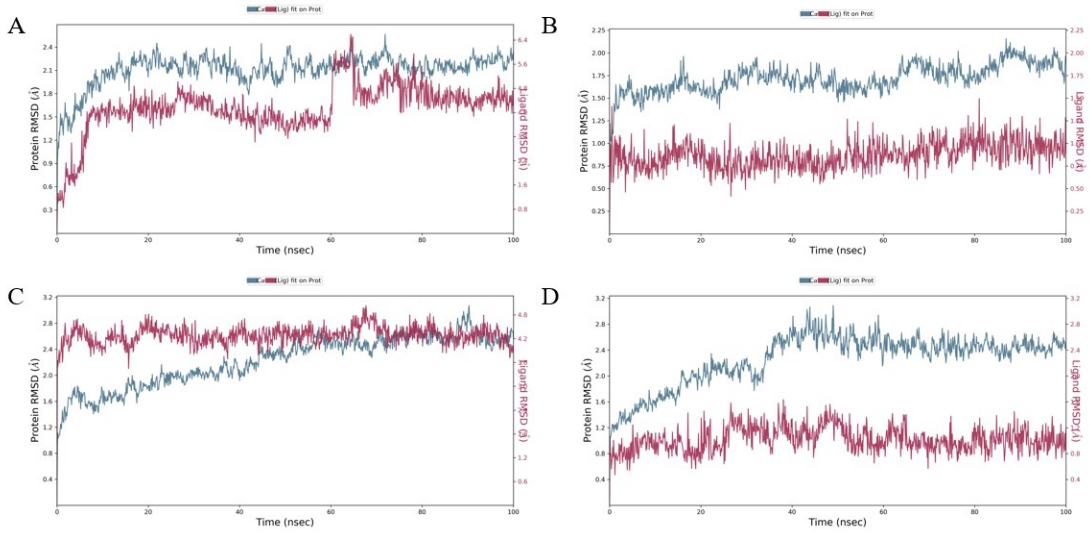

Figure S18 The RMSD plot of 5-HT_{2C}R protein with single residue mutated to alanine. (A) TYR118 mutated 5-HT_{2C}R/Pruvanserin complex. (B) LEU209 mutated 5-HT_{2C}R/Pruvanserin complex. (C) TYR118 mutated 5-HT_{2C}R/RS102221 complex. (D) LEU209 mutated 5-HT_{2C}R/RS102221 complex.

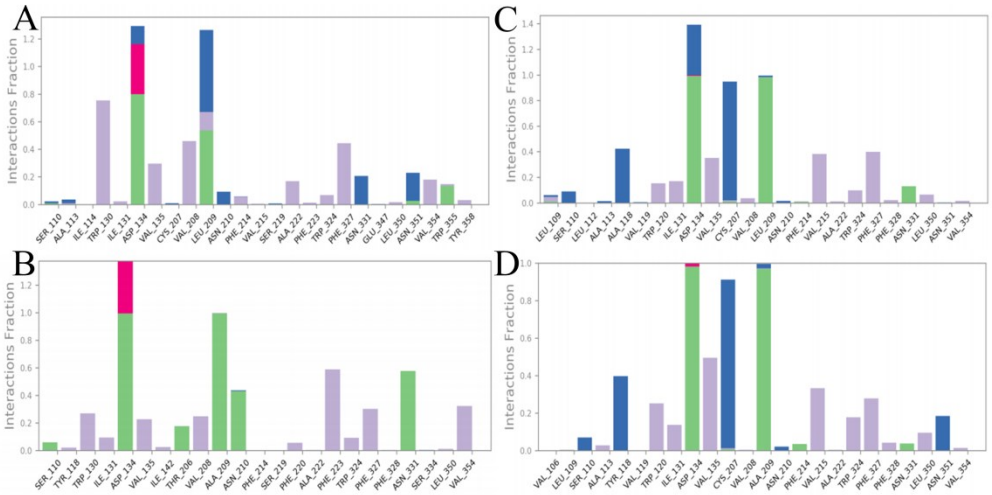

Figure S19 Normalized stacked bar charts of interactions and contacts throughout the course of MD simulations trajectory for mutated 5-HT_{2C}R complexes. (A) TYR118

mutated 5-HT_{2C}R/Pruvanserin complex. (B) LEU209 mutated 5-HT_{2C}R/Pruvanserin complex. (C) TYR118 mutated 5-HT_{2C}R/RS102221 complex. (D) LEU209 mutated 5-HT_{2C}R/RS102221 complex.

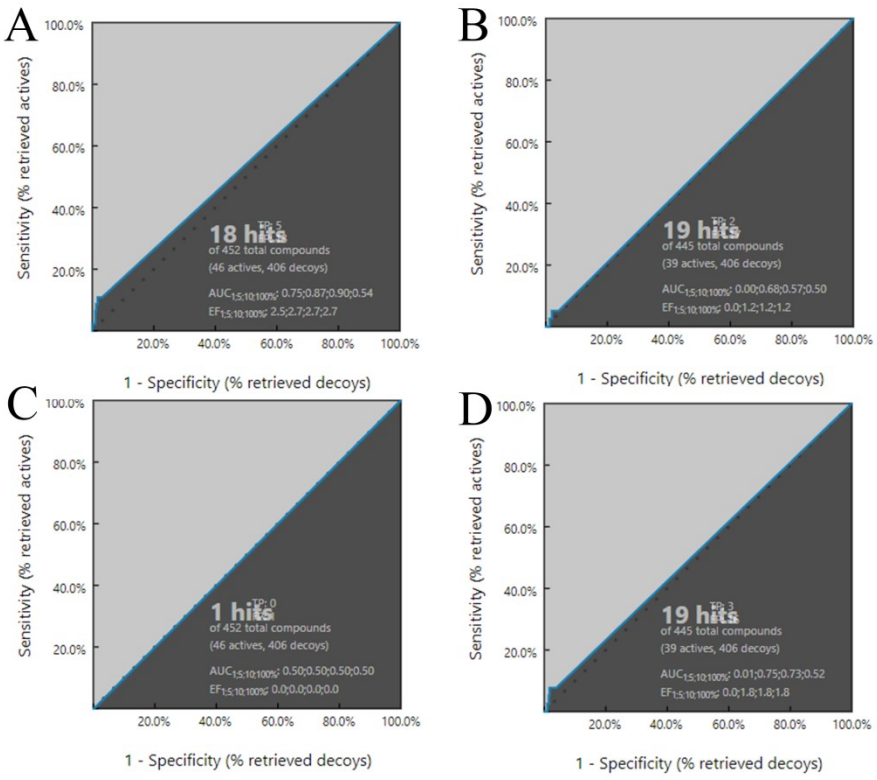

Figure S20 The ROC curves and AUC resulting from the evaluation of the structure-based pharmacophore models generated from the investigated 5-$HT_{2A/C}$R complexes. (A) 5-HT_{2A}R/Pruvanserin, (B) 5-HT_{2C}R/Pruvanserin, (C) 5-HT_{2A}R/RS102221, and (D) 5-HT_{2C}R/RS102221 complexes.

Table S1 Glide docking scores of Pruvanserin and RS102221 against 5-HT_{2A}R and 5-HT_{2C}R for the three parallel experiments

Entry	Ki (nM)	XP GScore (kcal mol^{-1})	Glide energy (kcal mol^{-1})	Glide emodel (kcal mol^{-1})
6A94/Pruvanserin	0.480 nM	-11.327	-53.763	-87.188
		-11.327	-53.763	-87.188
		-11.327	-53.763	-87.188
6A94/RS102221	2880nM	-4.765	-19.582	-30.773
		-4.765	-19.582	-30.773
		-4.765	-19.582	-30.773
6BQH /Pruvanserin	645 nM	-5.882	-47.137	-76.131
		-5.882	-47.137	-76.131
		-5.882	-47.137	-76.131
6BQH /RS102221	0.600 nM	-9.561	-55.368	-87.101
		-9.303	-48.8	-78.909
		-9.303	-48.8	-78.909